Human Gene Therapy

DOI: 10.1089/hum.2017.054

The Hydrophobic Effect from Conjugated Chemicals or Drugs on *in Vivo* Biodistribution of RNA Nanoparticles

*Daniel L. Jasinski, Hongran Yin, Zhefeng Li, and Peixuan Guo**

College of Pharmacy, Division of Pharmaceutics and Pharmaceutical Chemistry; College of Medicine, Department of Physiology & Cell Biology; Dorothy M. Davis Heart and Lung Research Institute; NCI Comprehensive Cancer Center; and Center for RNA Nanobiotechnology and Nanomedicine, The Ohio State University, Columbus, Ohio, USA.

Keywords: RNA nanoparticles, pRNA 3WJ motif, Nanobiotechnology, Biodistribution, Nanoparticle properties

***Address correspondence to:**

Peixuan Guo, Ph.D
Sylvan G. Frank Endowed Chair in Pharmaceutics and Drug Delivery
The Ohio State University
418 Biomedical Research Tower (BRT), 460 W 12th Ave.
Columbus, OH 43210, USA
Phone: 614-293-2114
Email: guo.1091@osu.edu

Human Gene Therapy
The Hydrophobic Effect from Conjugated Chemicals or Drugs on in Vivo Biodistribution of RNA Nanoparticles (DOI: 10.1089/hum.2017.054)
This paper has been peer-reviewed and accepted for publication, but has yet to undergo copyediting and proof correction. The final published version may differ from this proof.

ABSTRACT

Liver or other organ accumulation of drugs is one of the major problems that leads to toxicity and side effects in therapy using chemicals or other macromolecules. It has been shown that specially designed RNA nanoparticles can specifically target cancer cells, silence oncogenic genes, and stop cancer growth with little or no accumulation in the liver or other vital organs. It is well known that physical properties of nanoparticles such as size, shape, and surface chemistry affect biodistribution and pharmacokinetic profiles *in vivo*. In this study, we examined how the hydrophobicity of chemicals conjugated to RNA nanoparticles affect *in vivo* biodistribution. Weaker organ accumulation was observed for hydrophobic chemicals after they were conjugated to RNA nanoparticles, revealing RNA's ability to solubilize hydrophobic chemicals. We found that different chemicals conjugated to RNA nanoparticles resulted in the alteration of RNA hydrophobicity. Stronger hydrophobicity induced by chemical conjugates resulted in higher accumulation of RNA nanoparticles in vital organs in mice. This study provides new insights for handling drug insolubility, therapeutic toxicity, and organ clearance in drug development.

Human Gene Therapy
The Hydrophobic Effect from Conjugated Chemicals or Drugs on in Vivo Biodistribution of RNA Nanoparticles (DOI: 10.1089/hum.2017.054)
This paper has been peer-reviewed and accepted for publication, but has yet to undergo copyediting and proof correction. The final published version may differ from this proof.

INTRODUCTION

Interactions of nanoparticles with their *in vivo* environment is an important factor and affects nanoparticle characteristics such as protein binding, toxicity, pharmacokinetics, and biodistribution [1-8]. Accumulation of nanoparticles in healthy organs, such as the liver, kidneys, spleen, and lungs can lead to toxicity and lower efficacy of the administered dose of nanoparticles. While researchers are attempting to overcome this challenge with myriad of different nanoparticle systems, generally, less than 2% of the administered dose reaches the treatment site with the remaining dose sequestered by filtration organs, which leads to toxicity and off-target drug effects [4].

Recently, RNA nanoparticles have seen increased use as an *in vivo* delivery system [9-16]. Additionally, RNA based nanoparticles have been engineered to diverse shapes and sizes to carry multiple functionalities with unique release mechanisms [17-30]. RNA was once thought to have little potential for *in vivo* use due to biological and thermodynamic stability issues. However, these issues have been solved systematically by: (1) Finding of a thermodynamically stable three-way junction (3WJ) motif [9]; (2) Findings that chemical modifications to RNA nanoparticles confer enzymatic stability *in vivo* [31-34]; and (3) Finding that RNA nanoparticles exhibit little to no immunogenicity *in vivo* [19]. RNA nanoparticles are also water soluble and anionic due to the charged phosphate backbone. RNA nanoparticles show no accumulation in healthy organs, navigating to tumors after four hours of circulation [9-12,35-38].

It is well known that a nanoparticle's size, shape, and physical properties affects their interactions and biodistribution *in vivo*, and will therefore play a large role in determining their pharmacokinetics and biodistribution[2,39,40]. Thus, tremendous efforts have been made by nanoparticle engineers to overcome inherent downfalls in nanoparticle construction. For example, polyethylene glycol (PEG) is frequently used to increase water solubility of otherwise insoluble nanoparticles [41,42].

Conjugation of chemicals, such as fluorophores, drugs, and targeting ligands, is a popular method to decorate nanoparticles with functional moieties. However, many studies using hydrophobic fluorophores show nanoparticle accumulation in vital organs such as the liver, kidneys, lung, and spleen [43-47]. It is possible that the hydrophobic conjugates, in this case fluorophores, are promoting interaction with cell membranes and plasma proteins, causing

Human Gene Therapy
The Hydrophobic Effect from Conjugated Chemicals or Drugs on in Vivo Biodistribution of RNA Nanoparticles (DOI: 10.1089/hum.2017.054)
This paper has been peer-reviewed and accepted for publication, but has yet to undergo copyediting and proof correction. The final published version may differ from this proof.

accumulation of the nanoparticles in organs. In order for a nanoparticle to display low toxicity and low accumulation in vital organs, it is important to understand how conjugation of chemicals to nanoparticles affects their *in vivo* properties.

Previous *in vivo* studies using pRNA nanoparticles were carried out using charged and water soluble fluorophores to make sure the properties of the nanoparticles were not changed drastically [9-11,48]. However, as RNA nanotechnology progresses it will be important to know to what extent an RNA nanoparticle can be decreased in water solubility before accumulating in vital organs. Many potential applications such as chemical drug delivery and ligand based targeting involve conjugation of chemical groups to RNA nanoparticles, and many near-infrared fluorophores are hydrophobic potentially causing organ accumulation[43-47]. Additionally, toxicity and lower therapeutic effect of certain drugs, such as Taxol, has been correlated to their insolubility. When chemicals are conjugated externally and not encapsulated, the impact of the conjugate is likely to be more significant.

To investigate this, three fluorophores of different hydrophobicities were conjugated to the 3WJ RNA nanoparticle to serve as model chemicals: Cyanine5.5 (C5.5); Sulfonated-Cyanine 5.5 (SC5.5); and AlexaFluor700 (A700). All three fluorophores display similar excitation and emission spectra, despite minimal differences in their structures and solubility [49,50]. HPLC analysis demonstrated that conjugation of the fluorophores increased RNA nanoparticle hydrophobicity to differing extents. Hydrophobicity induced by chemical conjugates resulted in higher accumulation of RNA nanoparticles in vital organs of mice. Additionally, we observed weaker organ accumulation for hydrophobic chemicals after they were conjugated to RNA nanoparticles, suggesting that RNA can increase the solubility of hydrophobic chemicals. To offer a physical explanation for *in vivo* results, predictive compound logP (ClogP) values of the fluorophores and 3WJs were compared to experimentally determined hydrophobicity scales of amino acids, which are used to predict trans-membrane protein residues [51-54]. This study offers insight into drug development concerning the reduction of organ accumulation and drug toxicity or side effects of nanoparticles that are modified with chemical conjugates such as targeting ligands, fluorophores for tracking, and chemical drugs.

Human Gene Therapy
The Hydrophobic Effect from Conjugated Chemicals or Drugs on in Vivo Biodistribution of RNA Nanoparticles (DOI: 10.1089/hum.2017.054)
This paper has been peer-reviewed and accepted for publication, but has yet to undergo copyediting and proof correction. The final published version may differ from this proof.

MATERIALS AND METHODS

RNA Synthesis and Fluorophore Conjugation

RNA oligomers were chemically synthesized using typical phosphoramidite chemical synthesis on an automated oligo synthesizer. Sequences of the RNA oligomers used in biodistribution studies are as follows, listed in 5' to 3' orientation ("r" denotes 2'-OH base, "f" denotes 2'-F modified base). 3WJ-a: fUfUrGfUfCrAfUrGfUrGfUrAfUrG, 3WJ-b: fCrAfUrAfCfUfUfUrGfUfUrGrGfCfUrGrG, 3WJ-c: fCfCrArGfCfCrArAfUfCrAfUrGrGfCrArA. Following synthesis, oligomers were deprotected and desalted using conventional methods [55]. Each 3WJ strand was synthesized using 2'-fluorinated cytidine and uracil. 3WJ-c strand was 5' modified with a primary amine (Cat. No: 10-1947-90, Glen Research). Cyanine5.5-NHS ester and Sulfo-Cyanine5.5-NHS ester were purchases from Lumiprobe. AlexaFluor700-NHS Ester was purchased from Molecular Probes. Conjugation reactions were carried out by mixing a 1:10 molar ratio of primary amine labeled 3WJ-c: NHS Ester-Fluorophore in 0.1 M sodium bicarbonate buffer, pH = 8.5. The conjugation reactions were incubated at room temperature for 16 hours while protected from light. Following incubation, the reactions were ethanol precipitated and washed twice with cold 75% ethanol to remove the majority of unreacted fluorophore, facilitating purification.

HPLC Purification and Analysis of RNA-Fluorophore Conjugates

Samples were purified using IPRP-HPLC. Due to different hydrophobicities of each RNA-fluorophore conjugate, different HPLC gradient methods were used for each conjugate. Buffer A was 0.1 M triethylamine acetate (TEAA) (Glen Research) in water and buffer B was 0.1 M TEAA in 75% acetonitrile and 25% water. All purifications were performed using an Agilent 1260 HPLC and Agilent PLRP-S HPLC column (Agilent Cat. No: PL1512-5500). A flow rate of 1.5 mL/min was used throughout all HPLC methods and absorbance was monitored at 260 nm (RNA), 675 nm (C5.5, SC5.5), and 700 nm (A700). 3WJ-c-C5.5 was purified by a 5-100% gradient of buffer B over 15 minutes. 3WJ-c-SC5.5 was purified by 5-18% gradient of buffer B over five minutes followed by an 18-39% gradient over 15 minutes. 3WJ-c-A700 was purified by 5-18% gradient of buffer B over five minutes followed by an 18-38% gradient over 15 minutes. Fractions were collected when RNA absorbance and fluorophore absorbance eluted simultaneously. After fraction collection, RNA-fluor conjugates were dried to completion under vacuum.

Human Gene Therapy
The Hydrophobic Effect from Conjugated Chemicals or Drugs on in Vivo Biodistribution of RNA Nanoparticles (DOI: 10.1089/hum.2017.054)
This paper has been peer-reviewed and accepted for publication, but has yet to undergo copyediting and proof correction. The final published version may differ from this proof.

For %ACN elution comparison, an identical gradient of 5-100% buffer B over 20 minutes was used to analyze 3WJ-fluorophore nanoparticles, 3WJ-c-fluorophore conjugates, and fluorophores. %ACN elution was calculated based on elution times of RNA oligoes or 3WJ complexes. Delay time was calculated by injection of an RNA sample in a high hydrophobic environment (100% acetonitrile) to prevent interaction with the column. The experimentally determined delay time was then subtracted from sample elution time, which was then used to calculate %ACN elution.

Chromatograms were plotted using OriginPro. Plots comparing 3WJ %ACN elution show 3WJ absorbance at 260 nm, 3WJ-Cy5.5 and 3WJ-SCy5.5 absorbance at 675 nm, and 3WJ-A700 absorbance at 700 nm. Comparison of %ACN elution of dye species were values taken from analysis chromatograms of dye species (**Supp Fig 1B, C, D**). Values were plotted and then slope determined using a linear fit.

Determination of Predictive ClogP Values

ChemDraw Professional 16 was used to predict ClogP values of amino acids, fluorophores, and nucleotide-fluorophore conjugates. Amino acids, fluorophores, and nucleotide-fluorophore conjugates were drawn with charges analogous to their charged state at physiological pH = 7.4. Only the side chains of the amino acids were used for predictive ClogP calculations. Predicted ClogP values of amino acid side chains were then plotted versus previously published hydrophobicity scales of amino acids [53,54,56,57]. Four different hydrophobicity scales were chosen for comparison (**Supp Fig 2**) and it was found that the Cornette hydrophobicity scale was the best match to predictive ClogP values. The Cornette scale is based on 28 published scales and demonstrates one of the best overall scales of amino acid hydrophobicity. High values indicate higher degree of hydrophobicity.

Next, ClogP values of C5.5, SC5.5, and mono, di, and trinucleotide derivatives of the fluorophores were predicted (**Supp Table 2**). The structure of A700 is proprietary, and no structural information was available, however, SC5.5 and A700 demonstrate similar hydrophobicity based on IPRP-HPLC.

Human Gene Therapy
The Hydrophobic Effect from Conjugated Chemicals or Drugs on in Vivo Biodistribution of RNA Nanoparticles (DOI: 10.1089/hum.2017.054)
This paper has been peer-reviewed and accepted for publication, but has yet to undergo copyediting and proof correction. The final published version may differ from this proof.

In vivo Biodistribution

Male BALB/c mice, 5-6 weeks old, (Taconic) were injected intravenously (IV) through the eye using retro-orbital injection[58]. At 1, 4, and 8 hours mice were sacrificed and their hearts, kidneys, livers, spleen, and lungs collected and imaged for Cy5.5, SCy5.5, and A700 fluorescent signal using an *In Vivo* Imaging System (IVIS) imager (Caliper Life Sciences). Mice were administered PBS as a blank control. 100 μL of 20 μM nanoparticle sample or dye sample were injected. It is important to note that the concentrations of dyes was kept consistent in all *in vivo* experiments. All animal experiments were housed and performed in accordance with the Subcommittee on Research Animal Care of the Ohio State University guidelines approved by the Institutional Review Board.

Atomic Force Microscopy Imaging

Specially modified mica surfaces (APS mica) were used. The APS mica was obtained by incubation of freshly cleaved mica in 167nM 1-(3-aminopropyl) silatrane following previously reported protocol [59]. The RNA samples were diluted with 1 × TMS buffer to a final concentration of 3 - 5 nM. Then, 5-10 μL was immediately deposited on APS mica. After 2min incubation on the surface, excess samples were washed with DEPC treated water and dried under a flow of Argon gas. AFM images in air were acquired using MultiMode AFM NanoScope IV system (Veeco/Digital Instruments, Santa Barbara, CA) operating in tapping mode. The 3WJ nanoparticles used for AFM imaging only included 60 base pair extensions in order to better visualize the nanoparticles. Please refer to sequence information listed in the RNA Synthesis methods section for sequence information of RNA nanoparticles used in biodistribution studies.

RESULTS AND DISCUSSION

3WJ-fluorophore HPLC analysis

The 3WJ is composed of three component RNA oligomers: 3WJ-a, 3WJ-b, and 3WJ-c (**Fig 1A**). Mixing equimolar amounts of each component strand at room temperature in physiological buffer yields homogeneous RNA nanoparticles (**Fig 1B**) [9]. To fluorescently label the 3WJ

Human Gene Therapy
The Hydrophobic Effect from Conjugated Chemicals or Drugs on in Vivo Biodistribution of RNA Nanoparticles (DOI: 10.1089/hum.2017.054)
This paper has been peer-reviewed and accepted for publication, but has yet to undergo copyediting and proof correction. The final published version may differ from this proof.

nanoparticles, NHS-Ester derivatives of C5.5, SC5.5, and A700 were conjugated to primary amine labeled 3WJ-c strand (**Fig 1C**). Fluorophore conjugated oligomers were purified from un-labeled RNA by IPRP-HPLC. Following assembly of fluorophore labeled 3WJ nanoparticles (3WJ-C5.5, 3WJ-SC5.5, 3WJ-A700), polyacrylamide (PAGE) gel analysis was used to determine assembly efficiency. A decrease in migration rate of fully assembled 3WJ nanoparticles compared to monomer and dimer species indicates successful formation at high yield (**Fig 2A**). Gels were stained with ethidium bromide (EB) for total RNA visualization followed by scanning for EB and fluorophore signal. Co-migration of EB and fluorophore signal indicates successful incorporation of fluorophore-labeled oligomers into 3WJ nanoparticles. Labeling only one of three strands was used to confirm that the particles were not dissociating *in vivo*. It has been shown previously that single stranded RNA is eliminated rapidly through the kidneys after intravenous (IV) injection[60,61].

3WJ particles were then analyzed by IPRP-HPLC to compare elution times and %ACN elution (**Fig 2B**). Supplemental Table 1 shows a summary of nanoparticle elution times and %ACN elution. There is a strong correlation between the number of charged sulfate groups per fluorophore and the %ACN elution. 3WJ-C5.5 has the highest %ACN elution of 46.39 followed by 3WJ-SC5.5 at 22.72% and finally 3WJ-A700 at 21.49%. 3WJ with no fluorophore eluted at 14.13 %ACN. HPLC analysis indicates that different chemicals conjugated to RNA nanoparticles will increase the nanoparticle's hydrophobicity to differing degrees.

RNA nanoparticles solubilize hydrophobic chemicals

The hydrophilic property of RNA nanoparticles enables them to solubilize many hydrophobic chemicals. IPRP-HPLC demonstrates an increase in solubility (decrease in %ACN elution) from fluorophore alone to 3WJ-c-fluorophore to 3WJ-fluorophore (**Supp Fig 1B-D**). Interestingly, we see a much larger decrease in %ACN elution for the hydrophobic Cy5.5 fluorophore than for both hydrophilic fluorophores, indicated by more negative slope for Cy5.5 (**Fig 3**). The effect of RNA nanoparticles increasing solubility is evidenced by decreased fluorescent signal in vital organs when comparing 3WJ-fluorophore to fluorophore alone (**Fig 4B**). Especially strong evidence supporting this fact is observed when comparing fluorescence in lung and liver tissue between mice injected with fluorophore alone and 3WJ-fluorophore nanoparticles (**Fig 5**). The fluorophores alone accumulate in vital organs after 4 h whereas 3WJ-fluorophores display lower fluorescence, especially with C5.5 and A700.

Human Gene Therapy
The Hydrophobic Effect from Conjugated Chemicals or Drugs on in Vivo Biodistribution of RNA Nanoparticles (DOI: 10.1089/hum.2017.054)
This paper has been peer-reviewed and accepted for publication, but has yet to undergo copyediting and proof correction. The final published version may differ from this proof.

However, despite the high overall hydrophilicity, we still see both increased %ACN elution and accumulation with hydrophobic cell membranes when using a hydrophobic conjugate. This once again leads us to believe that the conjugate itself is interacting with cell membranes, and if the interaction of the conjugate with the cell membrane is strong enough it can overcome the hydrophilic nature of the RNA nanoparticle and the anionic property of RNA. Thus, not only is the overall hydrophilicity of the nanoparticle important, but so are the specific surface properties of the nanoparticle.

Fluorophore hydrophobicity vs biodistribution

Following HPLC analysis, the fluorophores were injected retro-orbitally into mice and fluorescent signal was whole body imaged 1, 4, and 8 h post-injection. Mice were then sacrificed and their organs collected and imaged. Fluorescent imaging from whole body images show low signal for A700 and SC5.5 and higher signal for C5.5 (**Fig 4A**). Organ images of the mice injected with the fluorophores all show fluorescent signal after 8 h (**Fig 4B**). These observations correlate well with the increased hydrophobicity of C5.5 over both SC5.5 and A700.

3WJ-fluorophore hydrophobicity vs biodistribution

The *in vivo* properties of the 3WJ-fluorophore nanoparticles were analyzed by testing their biodistribution profiles in mice. Whole body images indicate faster clearance of 3WJ-SC5.5 and 3WJ-A700 compared to and 3WJ-C5.5 (**Fig 4**). 3WJ-C5.5 showed high fluorescent signal in the organs compared to mice injected with PBS as a blank, primarily accumulating in the liver and kidneys after 8 h (**Fig 4B**). 3WJ-SC5.5 does show fluorescence in organs after 8 h, albeit much less intense than observed for 3WJ-C5.5. 3WJ-A700 shows no fluorescence in organs after 8 h. These *in vivo* results demonstrate a strong correlation between the increased hydrophobicity of the fluorophore and increased accumulation of nanoparticles in organs. Furthermore, these results show the ability of the 3WJ nanoparticle to increase the solubility of the fluorophores as less accumulation in vital organs of 3WJ-fluor nanoparticles is seen when compared to fluorophores. This is evidenced when examining differences in lung and liver tissue between mice injected with fluors alone and with 3WJ-fluorophore (**Fig 5)**.

Human Gene Therapy
The Hydrophobic Effect from Conjugated Chemicals or Drugs on in Vivo Biodistribution of RNA Nanoparticles (DOI: 10.1089/hum.2017.054)
This paper has been peer-reviewed and accepted for publication, but has yet to undergo copyediting and proof correction. The final published version may differ from this proof.

Physical basis for hydrophobicity effect on biodistribution

After *in vivo* results, we sought a physical explanation for our observations. One likely explanation for accumulation of the nanoparticles is interaction with proteins and cell membranes *in vivo*. It is our hypothesis that the increased hydrophobicity of the fluorophores conjugated to the 3WJ nanoparticles initiates interaction with the hydrophobic regions of proteins and cell membranes, causing the nanoparticles to accumulate in organs. Many studies have been done on the hydrophobicity of proteins and how the amino acid arrangement creates pockets of hydrophobicity and hydrophilicity [51-54,56,57]. These studies have generated amino acid hydrophobicity scales, which are used to predict hydrophobic regions in proteins and determine trans-membrane protein regions.

We hypothesized that the increased hydrophobicity of 3WJ-C5.5 was increasing the strength of the interactions between the hydrophobic regions of proteins and cell membranes and the nanoparticles. Because the RNA nanoparticles are extremely hydrophilic with a hydrophobic fluorophore attached, we expect them to exhibit an amphipathic property. This is akin to trans-membrane proteins, which are amphipathic to cross cell membranes.

A logP (partition coefficient) value is the ratio of a compounds solubility in two immiscible solvents, normally octanol: water, and is a good indication of hydrophobicity. Additionally, logP values are useful in estimating the biodistribution of drugs. More hydrophobic logP values generally indicate accumulation of drugs in hydrophobic areas such as the lipid bilayers of cells, while more hydrophilic logP values indicates accumulation of drugs in hydrophilic regions such as blood serum [62]. A ClogP value uses experimentally determined logP values of small fragments, and then adds these values together with correction factors to obtain a ClogP value [63]. When dealing with complex molecules, such as those containing aromaticity, ClogP values tend to be quite accurate.

We chose the Cornette[53] hydrophobicity scale as we observed the best correlation between predicted ClogP values and Cornette values (**Fig 6A**). A dotted line represents a neutral value of 0. The ClogP values were then plotted alongside ClogP values of amino acids (**Fig 6B**). Interestingly, C5.5 displays a high ClogP value while SC5.5 displays an extremely low ClogP value. Only when C5.5 is in trinucleotide form does the ClogP value reduce to near zero. ClogP values beyond trinucleotide form could not be predicted due to the increased number of atoms and software limitations. However, we expect as more nucleotides are added (54 in one 3WJ nanoparticle), the ClogP value would drastically decrease.

Human Gene Therapy
The Hydrophobic Effect from Conjugated Chemicals or Drugs on in Vivo Biodistribution of RNA Nanoparticles (DOI: 10.1089/hum.2017.054)
This paper has been peer-reviewed and accepted for publication, but has yet to undergo copyediting and proof correction. The final published version may differ from this proof.

Importantly, comparison of the predicted ClogP values of the amino acids with the fluorophores and their nucleotide derivatives provides some insights into the effect of hydrophobicity on cell membrane interaction. We see a highly-correlated trend between high ClogP value and organ accumulation *in vivo*. We also see a highly-correlated trend between high ClogP value and high value in the Cornette hydrophobicity scale. This shows that conjugates with high predicted ClogP values conjugated to a nanoparticle may cause interaction with the cell membrane, much like trans-membrane proteins.

While this study uses fluorophores to demonstrate how hydrophobicity affects nanoparticles *in vivo*, we expect it to extend to other conjugates such as chemical drugs or targeting ligands. For future use, it will be beneficial to determine beforehand if a conjugate will or will not cause nanoparticles to accumulate non-specifically *in vivo*. It is possible that using a screening method, such as the one presented in this study, will greatly benefit nanoparticle engineers looking to optimize their nanoparticle's physical properties. Specifically, for RNA nanoparticles, it could be beneficial to use encapsulation methods to protect the hydrophobic molecules from strong interactions with cell membranes or other proteins [17].

CONCLUSIONS

Our study demonstrates a strong correlation between increased hydrophobicity of an external conjugate and increased accumulation of nanoparticles in vital organs. Comparison of ClogP values of C5.5, SC5.5, and A700 to amino acids showed a strong correlation between hydrophobic dyes, which accumulate *in vivo*, to amino acids that are commonly seen in hydrophobic regions of trans-membrane proteins. Our results demonstrate a method to pre-screen nucleic acid based nanoparticle conjugates for their hydrophobic properties using a common method of HPLC analysis. As shown here, careful consideration must be taken when choosing to externally conjugate chemical drugs, fluorophores, or targeting ligands to water soluble nanoparticles, as their effect on water-solubility, and in turn *in vivo* biodistribution, could be detrimental to the safety of patients in future clinical settings. This study offers some insight into drug development concerning the reduction of organ accumulation of nanoparticles and reduction of drug toxicity and side effects.

ACKNOWLEDGEMENTS

The research in P.G.'s lab was supported by NIH grants R01EB019036, U01CA151648 and U01CA207946. We thank Mario Vieweger and Daniel W. Binzel for their insight in manuscript preparation.

AUTHOR DISCLOSURE STATEMENT

P.G.'s Sylvan G. Frank Endowed Chair position in Pharmaceutics and Drug Delivery is funded by the CM Chen Foundation. PG is the consultant of Oxford Nanopore Technologies and Nanobio Delivery Pharmaceutical Co. Ltd, as well as the cofounder of Shenzhen P&Z Bio-medical Co. Ltd and its subsidiary US P&Z Biological Technology LLC.

Human Gene Therapy
The Hydrophobic Effect from Conjugated Chemicals or Drugs on in Vivo Biodistribution of RNA Nanoparticles (DOI: 10.1089/hum.2017.054)
This paper has been peer-reviewed and accepted for publication, but has yet to undergo copyediting and proof correction. The final published version may differ from this proof.

Human Gene Therapy
The Hydrophobic Effect from Conjugated Chemicals or Drugs on in Vivo Biodistribution of RNA Nanoparticles (DOI: 10.1089/hum.2017.054)
This paper has been peer-reviewed and accepted for publication, but has yet to undergo copyediting and proof correction. The final published version may differ from this proof.

Reference List

1. Gustafson HH, Holt-Casper D, Grainger DW. et al. Nanoparticle Uptake: The Phagocyte Problem. Nano Today 2015;10:487-510.

2. Dobrovolskaia MA, Shurin M, Shvedova AA Current understanding of interactions between nanoparticles and the immune system. Toxicol Appl Pharmacol 2016;299:78-89.

3. Sadauskas E, Danscher G, Stoltenberg M. et al. Protracted elimination of gold nanoparticles from mouse liver. Nanomedicine 2009;5:162-169.

4. Wilheml S, Tavares AJ, Dai Q. et al. Analysis of nanoparticle delivery to tumours. Nature Reviews Materials 2016;1:1-12.

5. Kim ST, Saha K, Kim C. et al. The role of surface functionality in determining nanoparticle cytotoxicity. Acc Chem Res 2013;46:681-691.

6. Moyano DF, Goldsmith M, Solfiell DJ. et al. Nanoparticle hydrophobicity dictates immune response. J Am Chem Soc 2012;134:3965-3967.

7. Huang X, Li L, Liu T. et al. The shape effect of mesoporous silica nanoparticles on biodistribution, clearance, and biocompatibility in vivo. ACS Nano 2011;5:5390-5399.

8. Gratton SE, Ropp PA, Pohlhaus PD. et al. The effect of particle design on cellular internalization pathways. Proc Natl Acad Sci U S A 2008;105:11613-11618.

9. Shu D, Shu Y, Haque F. et al. Thermodynamically stable RNA three-way junctions for constructing multifuntional nanoparticles for delivery of therapeutics. Nature Nanotechnology 2011;6:658-667.

10. Binzel D, Shu Y, Li H. et al. Specific Delivery of MiRNA for High Efficient Inhibition of Prostate Cancer by RNA Nanotechnology. Molecular Therapy 2016;24:1267-1277.

11. Shu D, Li H, Shu Y. et al. Systemic delivery of anti-miRNA for suppression of triple negative breast cancer utilizing RNA nanotechnology. ACS Nano 2015;9:9731-9740.

Human Gene Therapy
The Hydrophobic Effect from Conjugated Chemicals or Drugs on in Vivo Biodistribution of RNA Nanoparticles (DOI: 10.1089/hum.2017.054)
This paper has been peer-reviewed and accepted for publication, but has yet to undergo copyediting and proof correction. The final published version may differ from this proof.

12. Cui D, Zhang C, Liu B. et al. Regression of gastric cancer by systemic injection of RNA nanoparticles carrying both ligand and siRNA. Scientific reports 2015;5:10726.

13. Shu Y, Haque F, Shu D. et al. Fabrication of 14 Different RNA Nanoparticles for Specific Tumor Targeting without Accumulation in Normal Organs. RNA 2013;19:766-777.

14. Afonin KA, Viard M, Koyfman AY. et al. Multifunctional RNA nanoparticles. Nano Lett 2014;14:5662-5671.

15. Roh YH, Deng JZ, Dreaden EC. et al. A Multi-RNAi Microsponge Platform for Simultaneous Controlled Delivery of Multiple Small Interfering RNAs. Angew Chem Int Ed Engl 2016;55:3347-3351.

16. Lee JB, Hong J, Bonner DK. et al. Self-assembled RNA interference microsponges for efficient siRNA delivery. Nat Mater 2012;11:316-322.

17. Khisamutdinov EF, Jasinski DL, Li H. et al. Fabrication of RNA 3D Nanoprism for Loading and Protection of Small RNAs and Model Drugs. Advanced Materials 2016;In Press:DOI: 10.1002/adma.201603180.

18. Khisamutdinov EF, Jasinski DL, Guo P RNA as a boiling-resistant anionic polymer material to build robust structures with defined shape and stoichiometry. ACS Nano 2014;8:4771-4781.

19. Khisamutdinov E, Li H, Jasinski D. et al. Enhancing immunomodulation on innate immunity by shape transition among RNA triangle, square, and pentagon nanovehicles. Nucleic Acids Res 2014;42:9996-10004.

20. Jasinski D, Khisamutdinov EF, Lyubchenko YL. et al. Physicochemically Tunable Poly-Functionalized RNA Square Architecture with Fluorogenic and Ribozymatic Properties. ACS Nano 2014;8:7620-7629.

21. Afonin KA, Desai R, Viard M. et al. Co-transcriptional production of RNA-DNA hybrids for simultaneous release of multiple split functionalities. Nucleic Acids Res 2014;42:2085-2097.

22. Afonin KA, Viard M, Martins AN. et al. Activation of different split functionalities on re-association of RNA-DNA hybrids. Nat Nanotechnol 2013;8:296-304.

Human Gene Therapy
The Hydrophobic Effect from Conjugated Chemicals or Drugs on in Vivo Biodistribution of RNA Nanoparticles (DOI: 10.1089/hum.2017.054)
This paper has been peer-reviewed and accepted for publication, but has yet to undergo copyediting and proof correction. The final published version may differ from this proof.

23. Grabow WW, Jaeger L RNA Self-Assembly and RNA Nanotechnology. Accounts of Chemical Research 2014;47:1871-1880.

24. Grabow WW, Zakrevsky P, Afonin KA. et al. Self-Assembling RNA Nanorings Based on RNAI/II Inverse Kissing Complexes. Nano Lett 2011;11:878-887.

25. Severcan I, Geary C, Chworos A. et al. A polyhedron made of tRNAs. Nat Chem 2010;2:772-779.

26. Afonin KA, Bindewald E, Yaghoubian AJ. et al. In vitro assembly of cubic RNA-based scaffolds designed in silico. Nat Nanotechnol 2010;5:676-682.

27. Chworos A, Severcan I, Koyfman AY. et al. Building programmable jigsaw puzzles with RNA. Science 2004;306:2068-2072.

28. Osada E, Suzuki Y, Hidaka K. et al. Engineering RNA-protein complexes with different shapes for imaging and therapeutic applications. ACS Nano 2014;8:8130-8140.

29. Boerneke MA, Dibrov SM, Hermann T Crystal-Structure-Guided Design of Self-Assembling RNA Nanotriangles. Angew Chem Int Ed Engl 2016;55:4097-4100.

30. Dibrov SM, McLean J, Parsons J. et al. Self-assembling RNA square. Proc Natl Acad Sci U S A 2011;108:6405-6408.

31. Liu J, Guo S, Cinier M. et al. Fabrication of stable and RNase-resistant RNA nanoparticles active in gearing the nanomotors for viral DNA packaging. ACS Nano 2011;5:237-246.

32. Veedu RN, Wengel J Locked nucleic acids: promising nucleic acid analogs for therapeutic applications. Chem Biodivers 2010;7:536-542.

33. Watts JK, Deleavey GF, Damha MJ Chemically modified siRNA: tools and applications. Drug Discovery Today 2008;13:842-855.

34. Somasunderam A, Thiviyanathan V, Tanaka T. et al. Combinatorial selection of DNA thioaptamers targeted to the HA binding domain of human CD44. Biochemistry 2010;49:9106-9112.

Human Gene Therapy
The Hydrophobic Effect from Conjugated Chemicals or Drugs on in Vivo Biodistribution of RNA Nanoparticles (DOI: 10.1089/hum.2017.054)
This paper has been peer-reviewed and accepted for publication, but has yet to undergo copyediting and proof correction. The final published version may differ from this proof.

35. Lee TJ, Haque F, Shu D. et al. RNA nanoparticles as a vector for targeted siRNA delivery into glioblastoma mouse model. Oncotarget 2015;6:14766-14776.

36. Zhang Y, Leonard M, Shu Y. et al. Overcoming Tamoxifen Resistance of Human Breast Cancer by Targeted Gene Silencing Using Multifunctional pRNA Nanoparticles. ACS Nano 2017;11:335-346.

37. Pi F, Zhang H, Li H. et al. RNA nanoparticles harboring annexin A2 aptamer can target ovarian cancer for tumor-specific doxorubicin delivery. Nanomedicine 2016;13:1183-1193.

38. Lee TJ, Yoo JY, Shu D. et al. RNA Nanoparticle-Based Targeted Therapy for Glioblastoma through Inhibition of Oncogenic miR-21. Mol Ther 2017.

39. Canton I, Battaglia G Endocytosis at the nanoscale. Chem Soc Rev 2012;41:2718-2739.

40. Arvizo RR, Miranda OR, Moyano DF. et al. Modulating pharmacokinetics, tumor uptake and biodistribution by engineered nanoparticles. PLoS ONE 2011;6:e24374.

41. He Q, Zhang Z, Gao F. et al. In vivo biodistribution and urinary excretion of mesoporous silica nanoparticles: effects of particle size and PEGylation. Small 2011;7:271-280.

42. Liu Y, Hu Y, Huang L Influence of polyethylene glycol density and surface lipid on pharmacokinetics and biodistribution of lipid-calcium-phosphate nanoparticles. Biomaterials 2011;35:3027-3034.

43. Owens EA, Hyun H, Dost TL. et al. Near-Infrared Illumination of Native Tissues for Image-Guided Surgery. J Med Chem 2016;59:5311-5323.

44. Porcu EP, Salis A, Gavini E. et al. Indocyanine green delivery systems for tumour detection and treatments. Biotechnol Adv 2016;34:768-789.

45. Wang F, Yang K, Wang Z. et al. Combined image guided monitoring the pharmacokinetics of rapamycin loaded human serum albumin nanoparticles with a split luciferase reporter. Nanoscale 2016;8:3991-4000.

46. Huynh AS, Estrella V, Stark VE. et al. Tumor Targeting and Pharmacokinetics of a Near-Infrared Fluorescent-Labeled delta-Opioid Receptor Antagonist Agent, Dmt-Tic-Cy5. Mol Pharm 2016;13:534-544.

Human Gene Therapy
The Hydrophobic Effect from Conjugated Chemicals or Drugs on in Vivo Biodistribution of RNA Nanoparticles (DOI: 10.1089/hum.2017.054)
This paper has been peer-reviewed and accepted for publication, but has yet to undergo copyediting and proof correction. The final published version may differ from this proof.

47. Pereira P, Correia A, Gama FM In Vivo Imaging of Glycol Chitosan-Based Nanogel Biodistribution. Macromol Biosci 2016;16:432-440.

48. Li H, Zhang K, Pi F. et al. Controllable Self-Assembly of RNA Tetrahedrons with Precise Shape and Size for Cancer Targeting. Adv Mater 2016;28:7501-7507.

49. Lumiprobe . Cyanine dyes.(https://www.lumiprobe.com/tech/cyanine-dyes). 2017. Ref Type: Abstract

50. Berlier JE, Rothe A, Buller G. et al. Quantitative comparison of long-wavelength Alexa Fluor dyes to Cy dyes: fluorescence of the dyes and their bioconjugates. J Histochem Cytochem 2003;51:1699-1712.

51. Silverman BD Hydrophobicity of transmembrane proteins: spatially profiling the distribution. Protein Sci 2003;12:586-599.

52. Rees DC, DeAntonio L, Eisenberg D Hydrophobic organization of membrane proteins. Science 1989;245:510-513.

53. Cornette JL, Cease KB, Margalit H. et al. Hydrophobicity scales and computational techniques for detecting amphipathic structures in proteins. J Mol Biol 1987;195:659-685.

54. Eisenberg D, Schwarz E, Komaromy M. et al. Analysis of membrane and surface protein sequences with the hydrophobic moment plot. J Mol Biol 1984;179:125-142.

55. Usman N, Ogilvie KK, Jiang MY. et al. The automated chemical synthesis of long oligoribuncleotides using 2'-O-silylated ribonucleoside 3'-O-phosphoramidites on a controlled-pore glass support: synthesis of a 43-nucleotide sequence similar to the 3'-half molecule of an Escherichia coli formylmethionine tRNA. J Am Chem Soc 1987;109:7845-7854.

56. Kyte J, Doolittle RF A simple method for displaying the hydropathic character of a protein. J Mol Biol 1982;157:105-132.

57. Engelman DM, Steitz TA, Goldman A Identifying nonpolar transbilayer helices in amino acid sequences of membrane proteins. Annu Rev Biophys Biophys Chem 1986;15:321-353.

58. Yardeni T, Eckhaus M, Morris HD. et al. Retro-orbital injections in mice. Lab Animal 2011;40:155-160.

59. Lyubchenko YL, Gall AA, Shlyakhtenko LS. et al. Atomic force microscopy imaging of double stranded DNA and RNA. J Biomol Struct Dyn 1992;10:589-606.

60. Behlke MA Chemical modification of siRNAs for in vivo use. Oligonucleotides 2008;18:305-319.

61. Behlke MA Progress towards in vivo use of siRNAs. Mol Ther 2006;13:644-670.

62. Shargel, L.; Susanna, W.; Yu, A. Chapter 10: Physiological Drug Distribution and Protein Binding. In *Applied Biopharmaceutics & Pharmacokinetics*, 6th ed.; McGraw-Hill Medical: New York, 2012; p 211.

63. Hansch, C.; Leo, A. Cpahter 5: Calculation of Octonal-Water Partition Coefficients from Fragments, etc. In *Substituent Constants for Correlation Analysis in Chemistry and Biology*, **John Wiley & Sons Ltd.**: New York, 1979.

Human Gene Therapy
The Hydrophobic Effect from Conjugated Chemicals or Drugs on in Vivo Biodistribution of RNA Nanoparticles (DOI: 10.1089/hum.2017.054)
This paper has been peer-reviewed and accepted for publication, but has yet to undergo copyediting and proof correction. The final published version may differ from this proof.

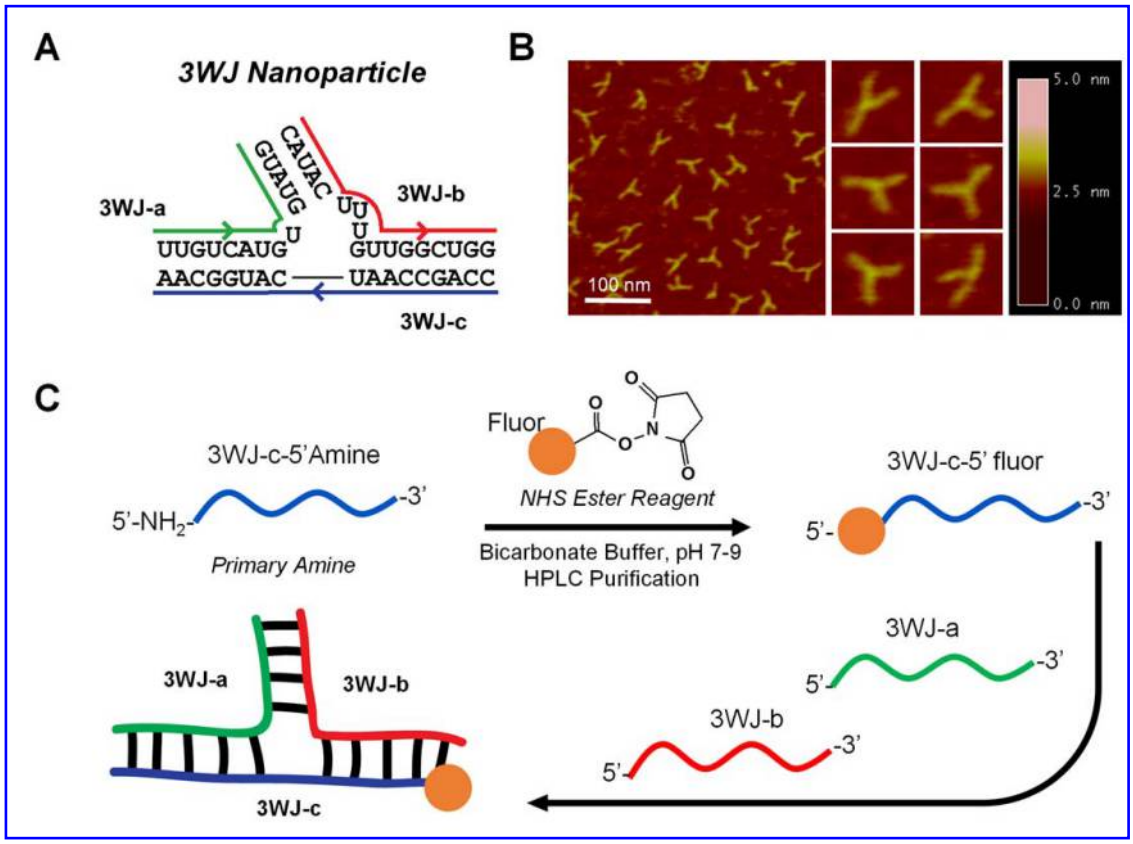

Figure 1. 3WJ Introduction and Dye Conjugation. (A) pRNA-3WJ secondary structure and sequences. **(B)** Atomic force microscopy images of pRNA-3WJ with 60 base pair extensions from each helix to show overall shape. **(C)** Assembly scheme of fluorescently labeled 3WJ nanoparticles.

Human Gene Therapy
The Hydrophobic Effect from Conjugated Chemicals or Drugs on in Vivo Biodistribution of RNA Nanoparticles (DOI: 10.1089/hum.2017.054)
This paper has been peer-reviewed and accepted for publication, but has yet to undergo copyediting and proof correction. The final published version may differ from this proof.

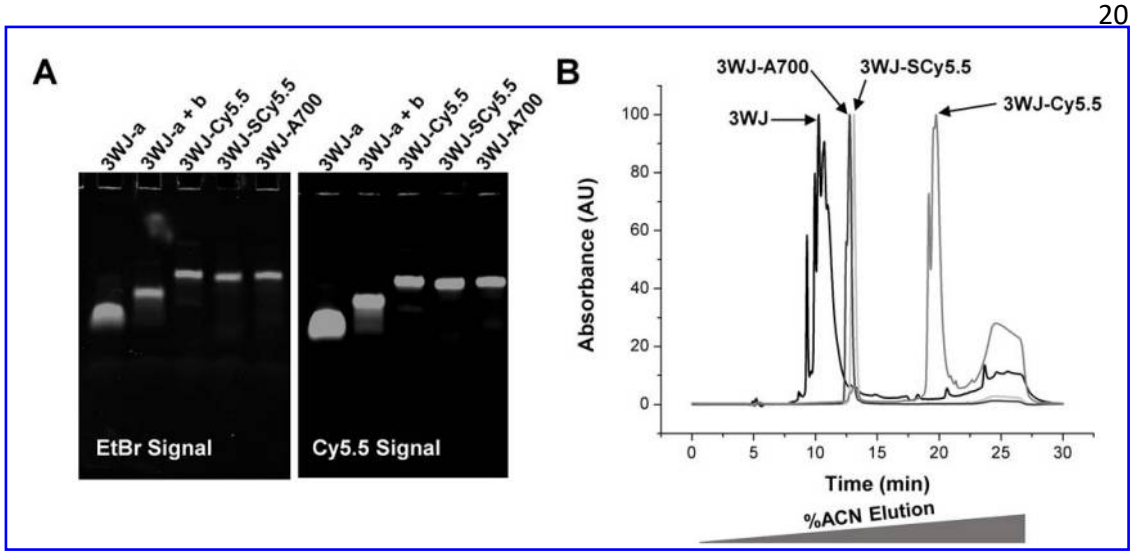

Figure 2. 3WJ Assembly and HPLC Analysis. (A) Native PAGE assembly gels of fluorescently labeled 3WJ nanoparticles. **(B)** IPRP-HPLC chromatograms of fluorescently labeled nanoparticles.

Human Gene Therapy
The Hydrophobic Effect from Conjugated Chemicals or Drugs on in Vivo Biodistribution of RNA Nanoparticles (DOI: 10.1089/hum.2017.054)
This paper has been peer-reviewed and accepted for publication, but has yet to undergo copyediting and proof correction. The final published version may differ from this proof.

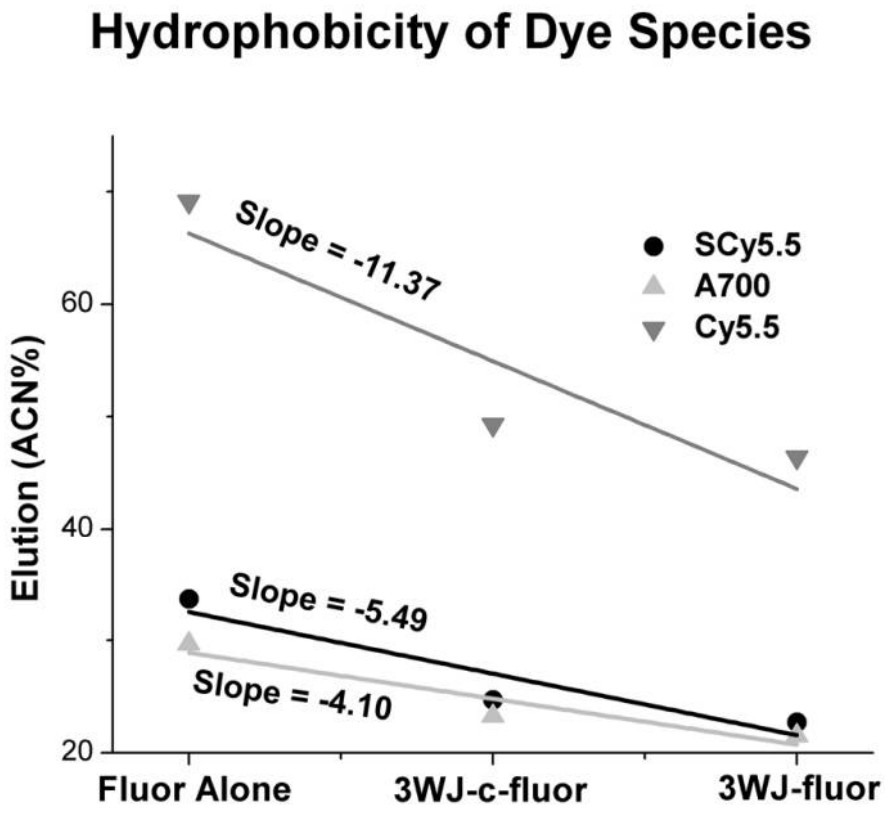

Hydrophobicity of Dye Species			
	Slope	Standard Error	R-Squared
Cy5.5	-11.37	4.88	0.69
SCy5.5	-5.49	2.01	0.76
A700	-4.10	1.34	0.81

Figure 3. Biodistribution in Mice. (A) Whole body fluorescent images of mice injected with fluors and 3WJ-fluors. **(B)** Organ images of mice IV injected with fluors and 3WJ-fluors.

Human Gene Therapy
The Hydrophobic Effect from Conjugated Chemicals or Drugs on in Vivo Biodistribution of RNA Nanoparticles (DOI: 10.1089/hum.2017.054)
This paper has been peer-reviewed and accepted for publication, but has yet to undergo copyediting and proof correction. The final published version may differ from this proof.

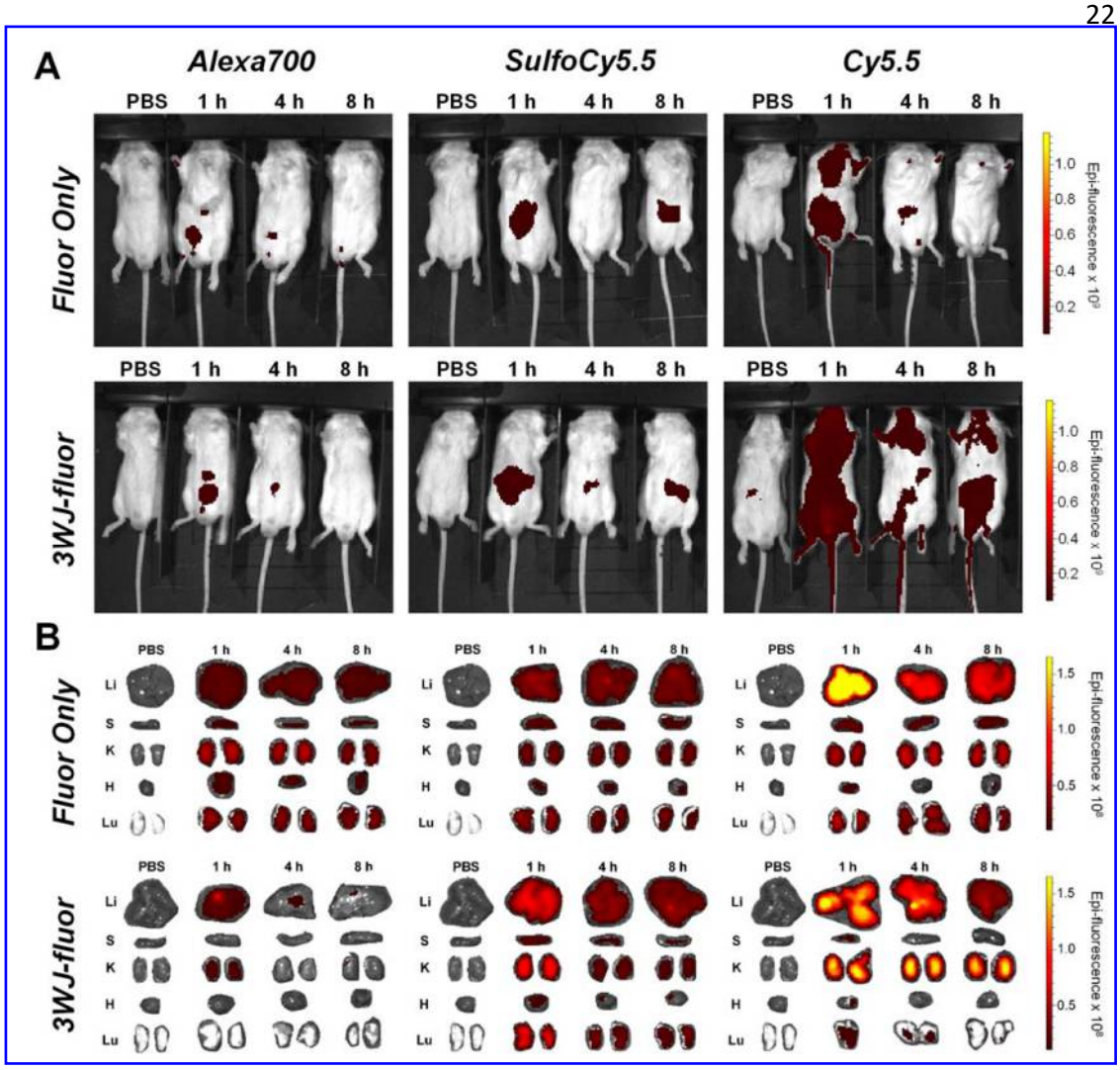

Fig 4. Fluor only vs 3WJ-fluor tissue comparison. Comparison of lung (Lu) and liver (Li) tissue collected from mice injected with fluorophores only or 3WJ-fluor conjugates after 4 and 8 hours.

Human Gene Therapy
The Hydrophobic Effect from Conjugated Chemicals or Drugs on in Vivo Biodistribution of RNA Nanoparticles (DOI: 10.1089/hum.2017.054)
This paper has been peer-reviewed and accepted for publication, but has yet to undergo copyediting and proof correction. The final published version may differ from this proof.

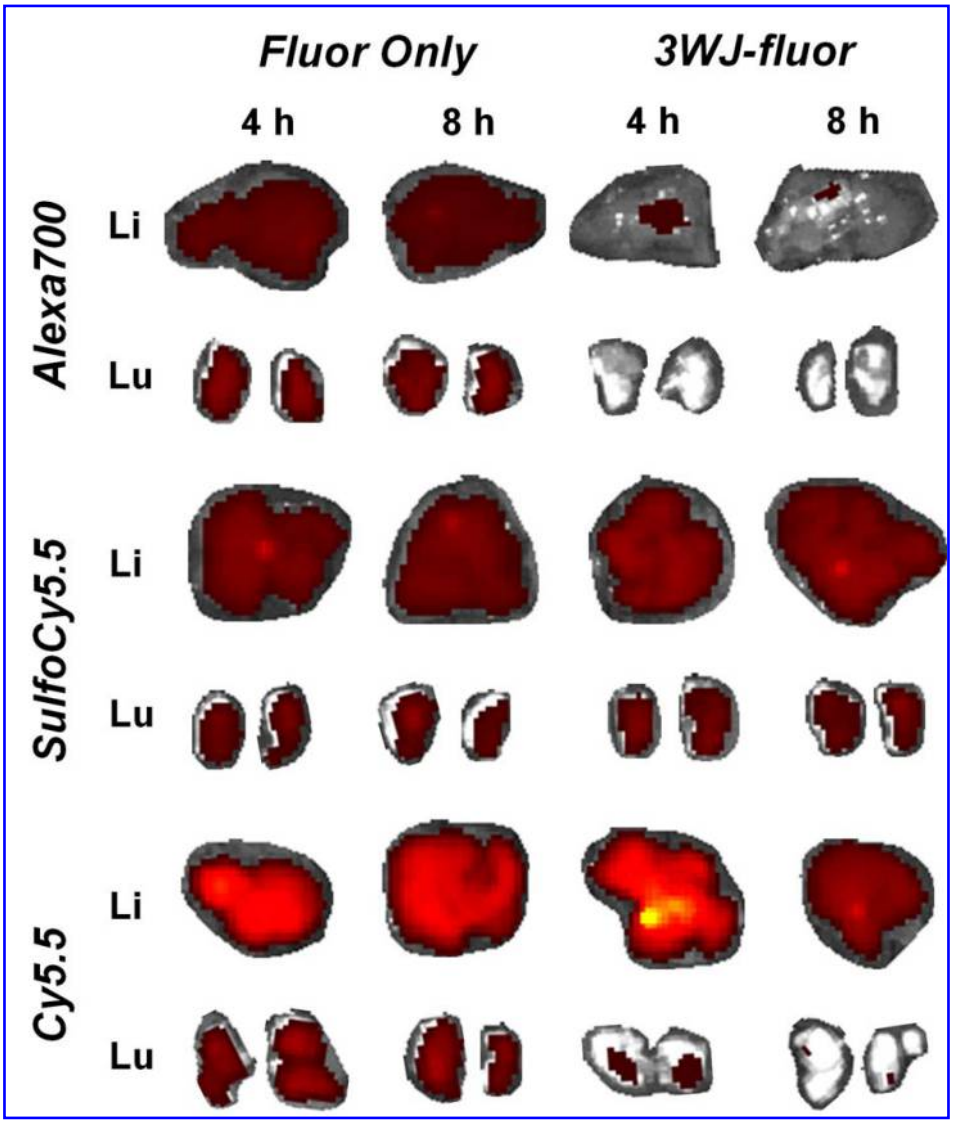

Figure 5. Hydrophobicity Comparison. (A) Plots of Cornette hydrophobicity scale values along with predicted ClogP values of the amino acids. **(B)** ClogP values were predicted for SulfoCy5.5 and their mono- and di-nucleotide derivatives, Cy5.5 and their mono- and di-nucleotide derivatives, and mono-, di-, and tri-nucleotides.

Human Gene Therapy
The Hydrophobic Effect from Conjugated Chemicals or Drugs on in Vivo Biodistribution of RNA Nanoparticles (DOI: 10.1089/hum.2017.054)
This paper has been peer-reviewed and accepted for publication, but has yet to undergo copyediting and proof correction. The final published version may differ from this proof.

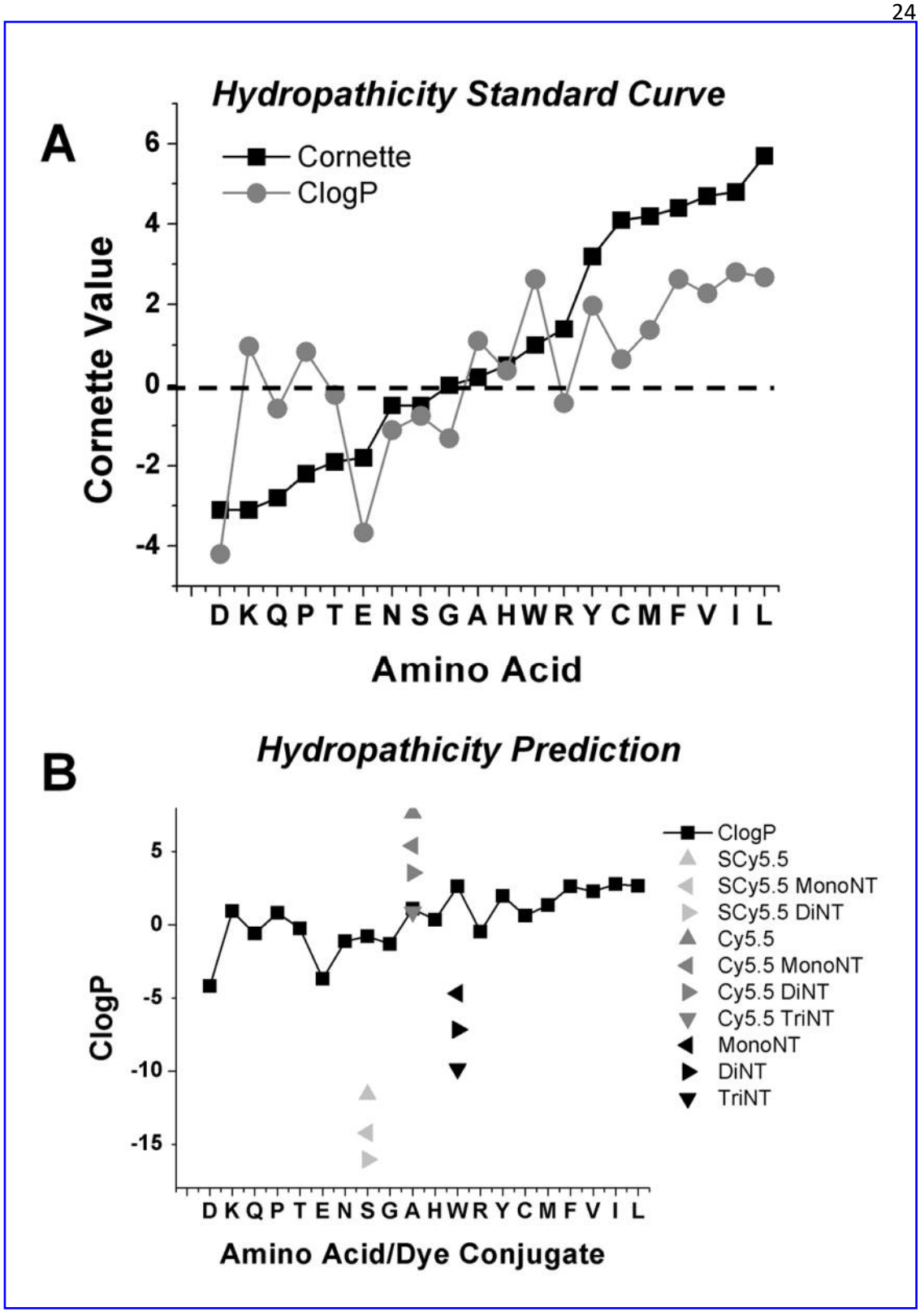

Figure 6. RNA nanoparticles solubilize hydrophobic chemicals. Three species of each fluorophore were plotted: fluorophore alone, 3WJ-c-fluorophore, and 3WJ-fluorophore for SulfoCy5.5, AlexaFluor700, and Cy5.5.

Human Gene Therapy
The Hydrophobic Effect from Conjugated Chemicals or Drugs on in Vivo Biodistribution of RNA Nanoparticles (DOI: 10.1089/hum.2017.054)
This paper has been peer-reviewed and accepted for publication, but has yet to undergo copyediting and proof correction. The final published version may differ from this proof.

Human Gene Therapy
The Hydrophobic Effect from Conjugated Chemicals or Drugs on in Vivo Biodistribution of RNA Nanoparticles (DOI: 10.1089/hum.2017.054)
This paper has been peer-reviewed and accepted for publication, but has yet to undergo copyediting and proof correction. The final published version may differ from this proof.

Supplementary Figure 1

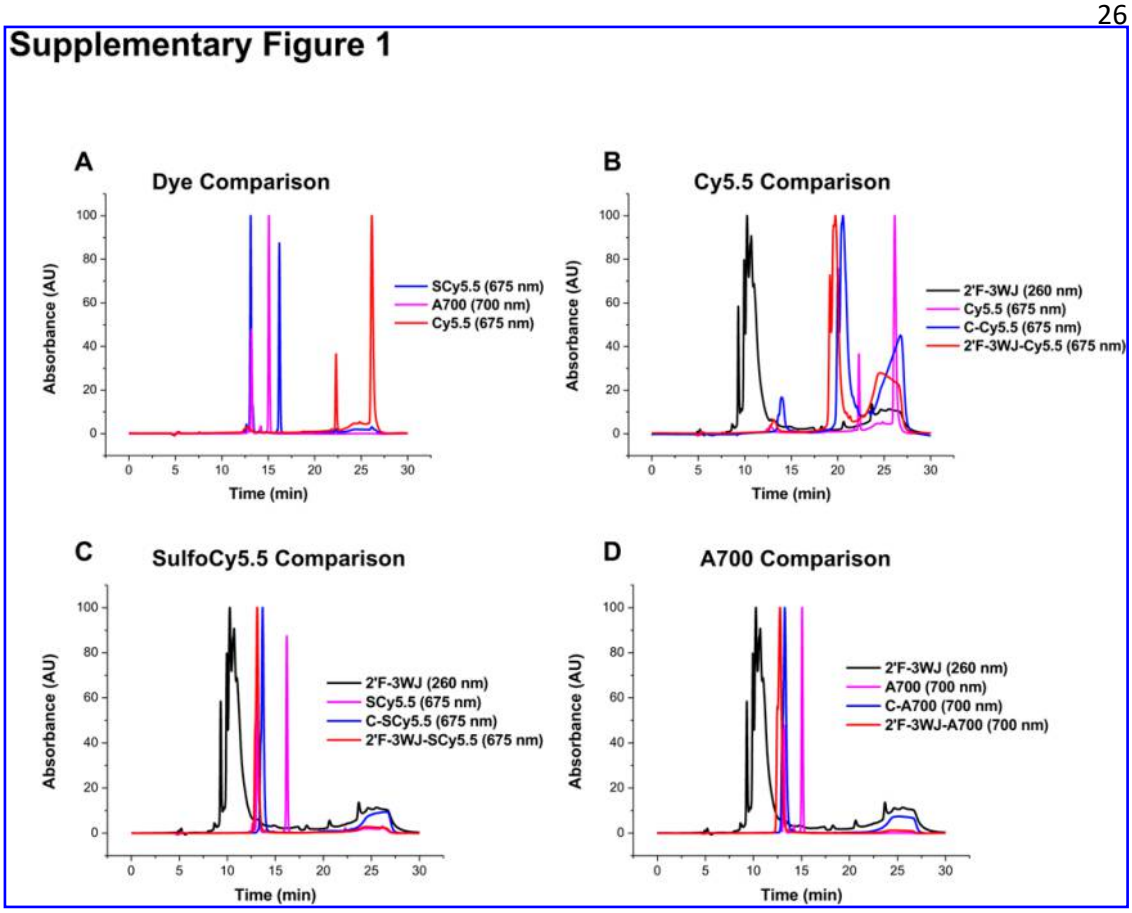

Human Gene Therapy
The Hydrophobic Effect from Conjugated Chemicals or Drugs on in Vivo Biodistribution of RNA Nanoparticles (DOI: 10.1089/hum.2017.054)
This paper has been peer-reviewed and accepted for publication, but has yet to undergo copyediting and proof correction. The final published version may differ from this proof.

Supplementary Figure 2

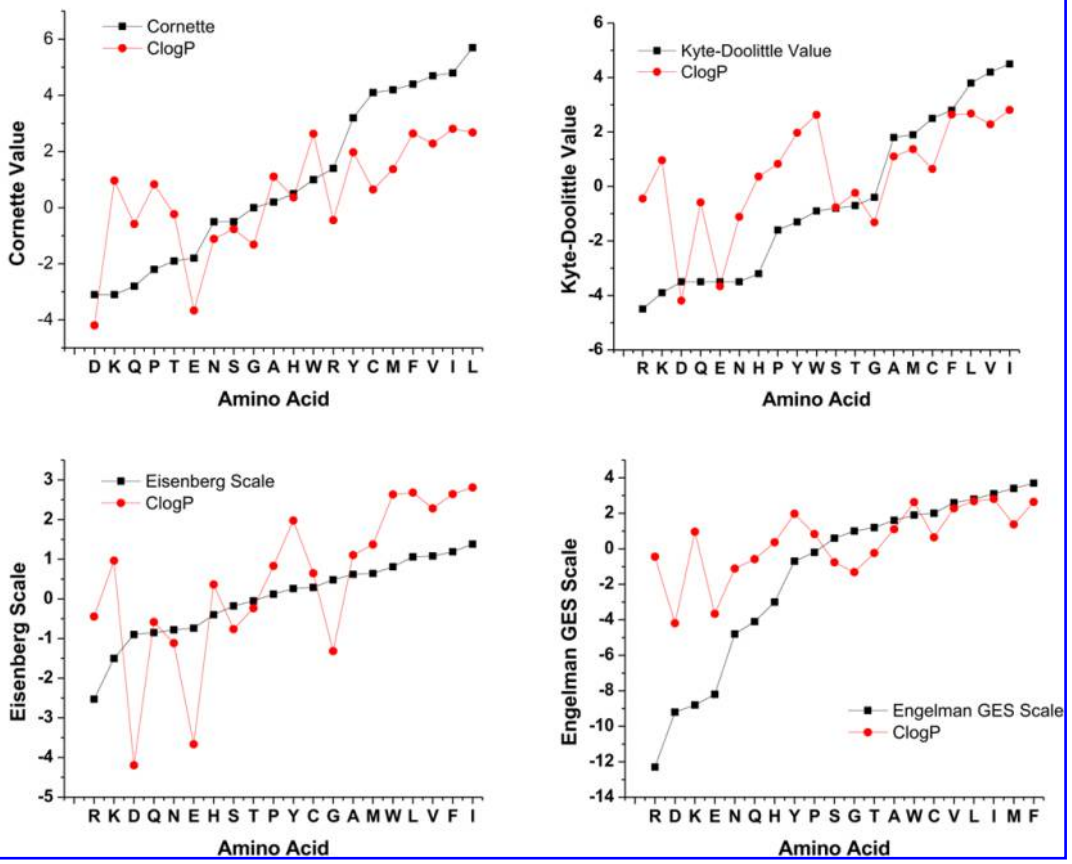

Human Gene Therapy
The Hydrophobic Effect from Conjugated Chemicals or Drugs on in Vivo Biodistribution of RNA Nanoparticles (DOI: 10.1089/hum.2017.054)
This paper has been peer-reviewed and accepted for publication, but has yet to undergo copyediting and proof correction. The final published version may differ from this proof.

Supplementary Figure 3

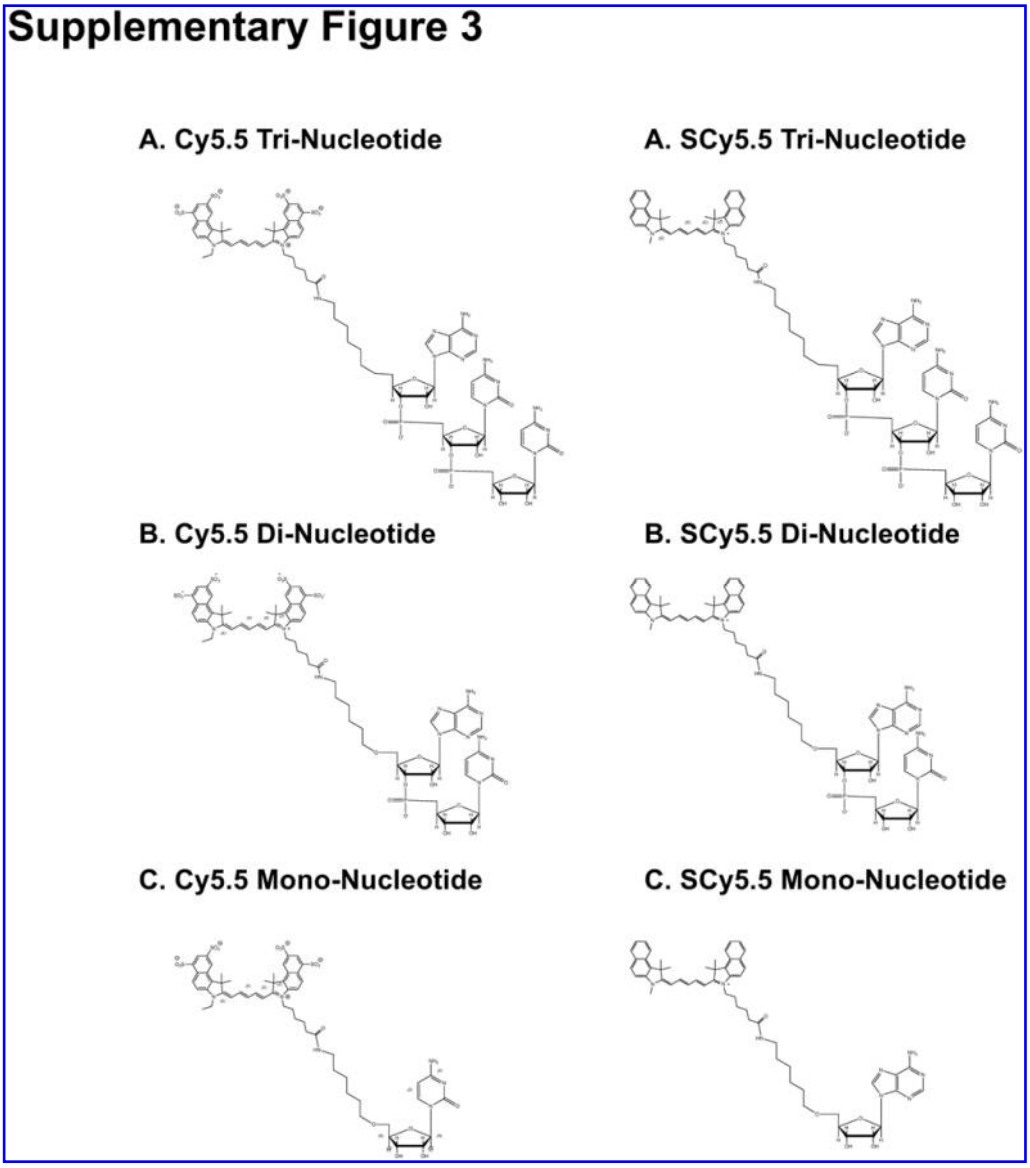

Human Gene Therapy
The Hydrophobic Effect from Conjugated Chemicals or Drugs on in Vivo Biodistribution of RNA Nanoparticles (DOI: 10.1089/hum.2017.054)
This paper has been peer-reviewed and accepted for publication, but has yet to undergo copyediting and proof correction. The final published version may differ from this proof.

Supplementary Table 1

RNA-Dye Conjugate	Elution Time (min)	%Acetonitrile Elution	In vivo Result	# of Sulfate Groups
Cy5.5	22.29/26.14	55.41/69.13	High in organs	0
SCy5.5	13.10/16.20	22.69/33.69	Low in organs	4
A700	13.19/15.07	22.97/29.68	Low in organs	?
2'F-3WJ-C	11.48	16.90	-	-
2'F-3WJ-C-Cy5.5	20.58	49.31	-	2
2'F-3WJ-C-SCy5.5	13.67	24.72	-	4
2'F-3WJ-C-A700	13.27	23.26	-	?
2'F-3WJ	10.70	14.13	-	-
2'F-3WJ-Cy5.5	19.76	46.39	High in organs	0
2'F-3WJ-SCy5.5	13.11	22.72	Low in organs	2
2'F-3WJ-A700	12.77	21.49	No Organs	?

Human Gene Therapy
The Hydrophobic Effect from Conjugated Chemicals or Drugs on in Vivo Biodistribution of RNA Nanoparticles (DOI: 10.1089/hum.2017.054)
This paper has been peer-reviewed and accepted for publication, but has yet to undergo copyediting and proof correction. The final published version may differ from this proof.

Supplementary Table 2

	Amino Acid	Cornette	ClogP	%ACN Elution
D	Aspartic Acid	-3.10	-4.19	-
K	Lysine	-3.10	0.96	-
Q	Glutamine	-2.80	-0.59	-
P	Proline	-2.20	0.83	-
T	Threonine	-1.90	-0.24	-
E	Glutamic Acid	-1.80	-3.67	-
N	Asparagine	-0.50	-1.11	-
S	Serine	-0.50	-0.76	-
G	Glycine	0.00	-1.32	-
A	Alanine	0.20	1.10	-
H	Histidine	0.50	0.36	-
W	Tryptophan	1.00	2.63	-
R	Arginine	1.40	-0.45	-
Y	Tyrosine	3.20	1.97	-
C	Cysteine	4.10	0.65	-
M	Methionine	4.20	1.37	-
F	Phenylalanine	4.40	2.64	-
V	Valine	4.70	2.28	-
I	Isoleucine	4.80	2.81	-
L	Leucine	5.70	2.68	-
	SCy5.5-NHS-Ester	-	-11.59	22.69/33.69
	SCy5.5-MonoNT	-	-14.22	-
	SCy5.5-DiNT	-	-16.06	-
	SCy5.5-TriNT	-	Highly Neg.	-
	Cy5.5-NHS-Ester	-	7.66	69.13
	Cy5.5-MonoNT	-	5.43	-
	Cy5.5-DiNT	-	3.59	-
	Cy5.5-TriNT	-	0.90	-
	A700-NHS	-	??	22.97/29.68
	MonoNT	-	-4.67	-
	DiNT	-	-7.16	-
	TriNT	-	-9.85	-
	3WJ-SCY5.5	-	Highly Neg.	22.72
	3WJ-Cy5.5	-	Neut to Neg.	46.39
	3WJ-A700	-	Highly Neg.	21.49